Optimising peak energy reduction in networks of buildings

Anush Poghosyan (ap647@bath.ac.uk)
University of Bath https://orcid.org/0000-0002-9400-1578
Nick McCullen
University of Bath https://orcid.org/0000-0002-7259-6320
Sukumar Natarajan
University of Bath https://orcid.org/0000-0001-5831-1678

Article

Keywords:

Posted Date: December 21st, 2021

DOI: https://doi.org/10.21203/rs.3.rs-783568/v2

Optimising peak energy reduction in networks of buildings

A. Poghosyan, N. McCullen, S. Natarajan

Department of Architecture and Civil Engineering, University of Bath, Claverton Down, Bath, BA2 7AY, UK

Keywords: complex networks, emergent behaviour, bio-inspired design, agent based modelling, Intelligent control, demand side management,

Abstract

Buildings are amongst the world's largest energy consumers and simultaneous peaks in demand from networks of buildings can decrease electricity system stability. Current mitigation measures either entail wasteful supply-side over-specification or complex centralised demand-side control. Here, we investigate a new schema for decentralised, self-organising building-to-building load coordination that requires very little information and no direct intervention. We find that the theoretically optimal size for load-coordination networks can be surprisingly small, analogous to other complex systems such as coordination between flocks of birds. The schema outperforms existing techniques, giving substantial peak-reductions as well as being remarkably robust to changes in other system parameters such as the network topology. This not only demonstrates that significant reductions in network peaks are achievable using remarkably simple control systems but also reveals theoretical results and new insights which which will be of great interest to the complexity and network science communities.

1. Introduction

We spend nine-tenths of our lives within buildings, relying on a consistent supply of energy to live and work well. Buildings therefore not only account for between 40–60% of global energy demand [1–6], but are also responsible for creating sharp peaks in demand in response to extreme heat or cold [7–9]. Recent examples—such as Texas' February 2021 blackout due to extreme cold, which left more than 10 million people without power for days [10], followed by a June 2021 blackout due to extreme heat—demonstrate the severe stress on energy networks emanating from unprecedented extreme events, which are only expected to increase in frequency and severity as the global climate warms [11–19]. Even predictable extremes are unsustainable in the long term, as they require fast-response fossil-fuel generators—known as "Peakers" in the U.S.,—which are expensive and opposed to the urgent need for carbon mitigation. As an example of its significance, just 1% of annual hours are responsible for between 10% and 20% of wholesale electricity costs in the U.S. [20], reflective of the need for more expensive and carbon-intensive peakers such as coal or gas fired generators.

Hence, it is of the utmost importance that energy systems are designed to be not only resilient, but cost-effective and carbon efficient, now and in the future. Since supply-side solutions can aid resilience, but are expensive [21] and result in greater carbon emissions [22, 23], focus has primarily been on demand-side strategies, which tackle the problem of peak demand at the building level. These include techno-economic strategies for dispatchable loads—those that can respond to changes in a short timescale of typically less than 30 minutes [24]—and tariff-driven strategies for non-dispatchable loads [25, 26]. Unfortunately, despite considerable recent interest, the maximum peak reduction of such strategies has been shown to be only around 5% [27]. The two main challenges in these strategies have been insufficient user-engagement to realise savings [27, 28] and the need to predict when loads might occur [24–26, 29–31]. The latter often relies on hard-to-obtain data—including appliance inventories, scheduling, the timing and size of actual loads, occupancy and localised weather—further complicating the prediction problem.

Another significant weakness of the vast majority of demand-side approaches is that they only consider how peak loads can be reduced at the level of an individual building. This means that it is possible for a given peak reduction measure to be simultaneously enacted by several buildings in the network – leading to new peaks and thus reducing the overall efficacy of the measure [32]. Given that the problem of peaks occurs due to a synchronisation of the *same type* of load across several buildings in a network, substantial peak

reductions could be achieved by considering how loads, especially those of a similar type, can be coordinated across groups of buildings.

Even techniques that approach the problem at group level usually centralise the optimisation and control schemes [24, 25, 31–36]. This imposes computational complexity complexity and a higher associate cost, which increases exponentially with the number of coordinated buildings [32], as identifying optima requires considering the entire search space [37]. This significantly limits the potential scale of application given that the number of buildings served by a single network end-point are usually at least an order of magnitude higher than can be studied effectively [38].

Hence, an ideal peak reduction system would be one that (i) allows decentralised load coordination between buildings such that the coincidence of identical loads is minimised (ii) is computationally simple (iii) is easily scalable to a large number of buildings (iv) has the potential to be low-cost and (v) requires little to no human intervention.

Nature shows that complex systems are often governed by interactions between small groups of individuals in a much larger system, and provides many powerful examples of how decentralised coordination between elements of a complex biological system – with no knowledge of the overall system's state or properties – can result in highly desirable "emergent" behaviour at system level [39, 40]. For example "birds" only interact with 6–7 other individuals in models of starling murmurations [41], with each obtaining real-time information only on the location and speed of its nearest neighbours [42]. While such bio-inspired approaches have been used to solve crowd disaster and pedestrian flows [43], collective learning [44] and flight formation control of air vehicles [45] problems, their applicability to the problem of energy demand management has previously not been studied, so their efficacy is not known.

Thus, a simple schema is developed here to study the best network and model parameters that could result in optimal behaviour, as well as the extent of peak load reduction that could be achieved through this type of decentralised self-organising load coordination between groups of buildings in a network. Dwellings are used as the buildings in the model due to their higher demand profile compared to non-dwellings and the fact they present a more significant coordination challenge due to the distributed nature of loads. The coordination schema is based around loads that are "shiftable" in time [46–48], as opposed to base loads (e.g., refrigerators) and on-demand loads (e.g., kettles). We also distinguish less-constrained shiftable loads, such as dishwashers, from more-constrained thermal loads for space heating or cooling requirements. This is an important distinction, often missing in the literature, as time-constrained thermal loads are also significantly larger than other loads, and their impact on network peaks is therefore more pronounced.

An agent-based model (ABM) framework was used to run a variety of simulations and determine which key parameters significantly influence the magnitude of any observed peak reductions arising from the schema. The factors investigated were group size, network topology, coordination time-scale and the size of load allowed to be redistributed in each time-step. Each of these factors represents a significant unknown that could affect the overall robustness of the system: for example large groups may prove harder to coordinate in practice, a single successful network topology could be less flexible than a multitude of topologies and longer coordination time-scales might negatively affect user-acceptance depending on the nature of the load.

2. Results

The goal in this work is to uncover the key factors influencing load coordination between buildings and if they are likely to result in substantial peak reduction. Since the interaction of buildings will occur via the links of the network connecting them, a range of network topologies were examined, with a view to investigate their impact on any resultant peak load reduction. Alongside this, the key parameters were investigated for a simple load coordination schema that requires little data or human intervention, relying on only simple rules and minimal interaction.

2.1. A simple schema for load coordination

The buildings or dwellings constitute the *nodes* on a network and are directly connected with others (their *network neighbours*) via information links (the *network edges*). Several common network topologies were investigated (described in §5.1). For the nodes to coordinate their demand, some information must be exchanged between groups of directly-connected nodes, termed the *neighbourhoods* of the nodes. This information is used to enable one of the following actions—if a suitable shiftable load has been requested for either now or is offset into a "demand pool" for later:

(i) consume a shiftable load now, to fill spare capacity – either on-demand or from the demand-pool;
(ii) delay the load until later, to reduce current demand;

This forms the minimal set of actions that a node-level agent in the network may take that should also be sufficient to flatten load profiles at the system level. While elaborations on these actions are possible—such as "consume x% less energy now" or "use appliance `x` but not `y`"—these can be considered semantic variations on the basic rules. For simplicity the actions are framed in terms of loads, even though energy consumption is in reality never a direct action but rather the result of some other action motivated by the needs and desires for daily living, such as turning on a heating system to increase comfort, watching television, or making tea [49].

For an agent to take one of the above actions it requires a knowledge of the current neighbourhood load compared to the maximum allowable load at any given time. This can then be used along with its own current and scheduled—i.e., previously unfulfilled—demand, to act to help reduce inter-building peaks. The maximum possible "network neighbourhood peak" is the likely peak load, defined as l_{max}, that might occur if all buildings within a neighbourhood were to demand all available loads simultaneously. In real settings, l_{max} could be estimated by an observation of peak loads for a defined neighbourhood over some arbitrary time-scale. Or, more simply, as the sum of the maximum load allowed by the service provider for each building. The minimum external information that needs to be transferred to each agent is therefore the load drawn by its neighbourhood at any given point in time. Hence we obtain a very simple definition of the information needed by each building for load coordination, involving just two aspects alongside its own demands: the likely neighbourhood peak l_{max} and the current load drawn by a given building's neighbours. Once again, this is analogous to the use of minimal information by individuals in animal collective behaviour—such as in models of flocking birds, where a given starling adjusts its own position and speed, based on the relative position of its nearest neighbours [42].

Once these simple pieces of information are known, the dwelling agent decides both: (a) whether to either delay load consumption to lower current demand or consume scheduled load to fill a gap in demand; and (b) how much load to shift if this is required. Both the threshold for the decision to shift loads and the amount of load to shift are determined as a proportion α of the permissible peak load (l_{max}). The control parameter α acts as a limit to the amount of demand a single actor can shift in one go and prevents multiple buildings inadvertently creating a new peak at the current time-step through coincident rescheduling. Section 5.4 explains how these features are implemented within the peak coordination algorithm.

The ideal network load would be a constant load profile, given by averaging the total network load (for all dwellings) in the network over the time interval being investigated. This is related to l_{max} in that the most extreme scenario would be where all neighbourhoods peak simultaneously, with each using all available loads at the same time. The root mean square error (RMSE) between a given load profile—generated by the ABM—and the ideal average network load is used to compare the un-adjusted load distributions to those using the peak coordination schema. Low values of the RMSE show that the corresponding load profile is close to the flat average network load – with a totally peak-free, flat profile having an RMSE of zero. In the presented results, the RMSE values are plotted as a function of the parameter α, to easily compare them with the other parameters investigated. Ramp-rates—i.e., the maximum rate of change of demand—are presented in half hour intervals, as this is a common network trading period, such as in the UK's national grid [50].

2.2. Simulation scenarios

The parametric investigation of our model is separated into two scenario groups (shown in Table 1 in §5.3), with Scenario Group 1 having a fixed number of directly linked neighbours (average node degree) but variable time windows for demand shifting and Scenario Group 2 having a range of degrees but fixed time shifting window.

2.2.1. Impact of time shifting window

Detailed analysis of the model outputs shows that for all network topologies, the peak reduction schema is most effective (i.e., achieves the most peak load flattening) when the load redistribution limit $\alpha \approx 15\%$ and the time shifting window is equal to 6 hours. For example, in the network with partition topology shown in Figure 1 the lowest RMSE is recorded for when the time shifting window is 6 hours (RMSE = 0.46). Time

shifting windows of 3 and 12 hours lead to higher RMSE values of 0.57 and 0.65 respectively. The RMSE values shown in Figure 1 illustrate the dependence of the effectiveness of the peak reduction schema on both the time shifting window and load redistribution limit α. Scenarios where $\alpha = 1$ or $\alpha = 0$ are where all agents in a neighbourhood end up following the same tactic, which results in peak demand shifting from one point of time to another or remaining the same with no flattening achieved. This is equivalent to a peak reduction strategy that operates solely at the individual building level.

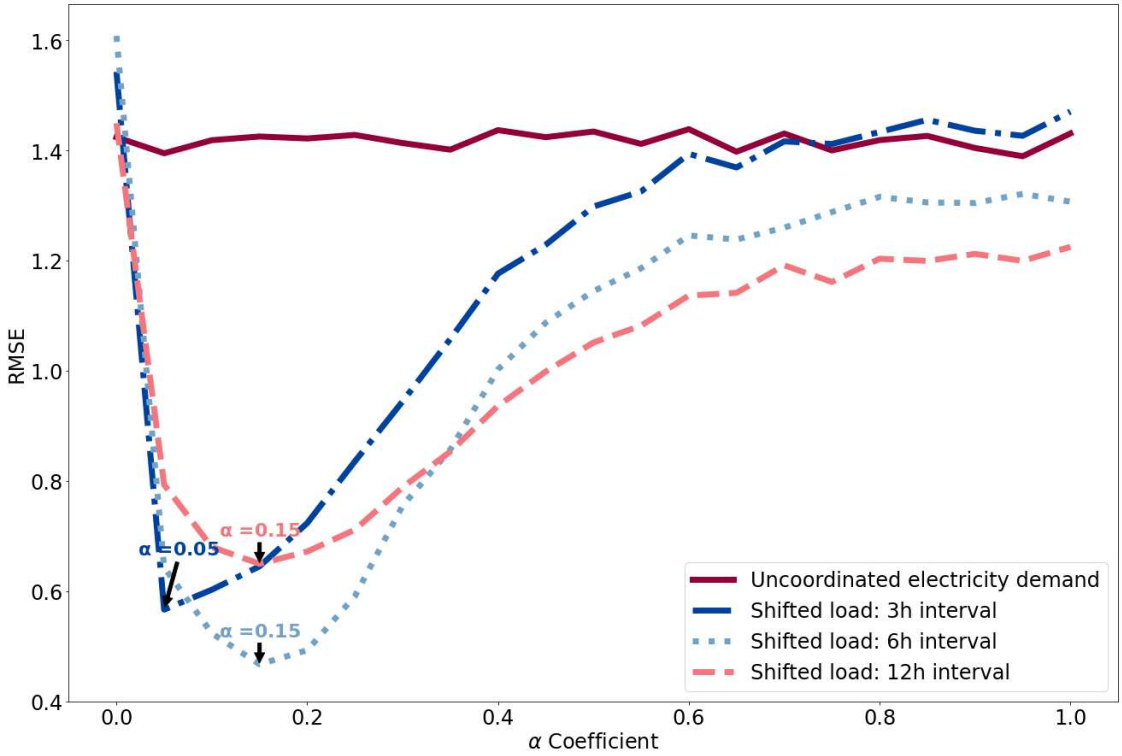

Figure 1. Partition network ($d = 4$): impact of time shifting window on peak control and reduction. Results obtained using different network topologies appear almost identical. The minima of the three shifted curves are indicated by arrows at $\alpha = 0.050$, $\alpha = 0.15$ and $\alpha = 0.15$ for the 3h, 6h and 12h shifting interval, respectively.

It is pertinent to observe that, while clear minima in RMSE are identified at a particular load distribution limit, the width of a given curve indicates the robustness of the different configurations. That is, the less steep the trough of a curve, the more robust the given configuration to produce lower peak demand.

2.2.2. The impact of network topology and node degree

Results from Group 2 in Figure 2 show that, surprisingly, network topology does not significantly influence the peak reduction behaviour of the implemented peak coordination schema. This is demonstrated by simulation outputs under scenarios with very different network topologies showing strikingly similar RMSE values for each α, as seen in the relatively narrow coloured envelopes for each set in Figure 2. The partition and ring lattice topologies are particularly close, and whilst the RMSEs from random network topologies differ slightly from those of the partition and random "small-world" Watts-Strogatz (WS, $p = 0$) topologies. These are not significant and likely due to the variation in node degrees inherent in such random networks.

The most interesting result here is the impact of average node-degree (see §5.1.1), i.e., number of neighbours, on peak demand reduction. While all node-degrees share similar RMSE minima, their gradients increase more steeply with higher node-degree as α increases. The width of our curves can be compared using the well-known full width half maximum (FWHM) bandwidth, which reveal that, for all network topologies, RMSE curves for average node degree 2 are approximately twice the width of those with average degrees 8 and 10. However, the FWHM widths for networks with average node degrees 8 and 10 do not show any significant differences. This indicates that our peak coordination schema is most robust over a broad

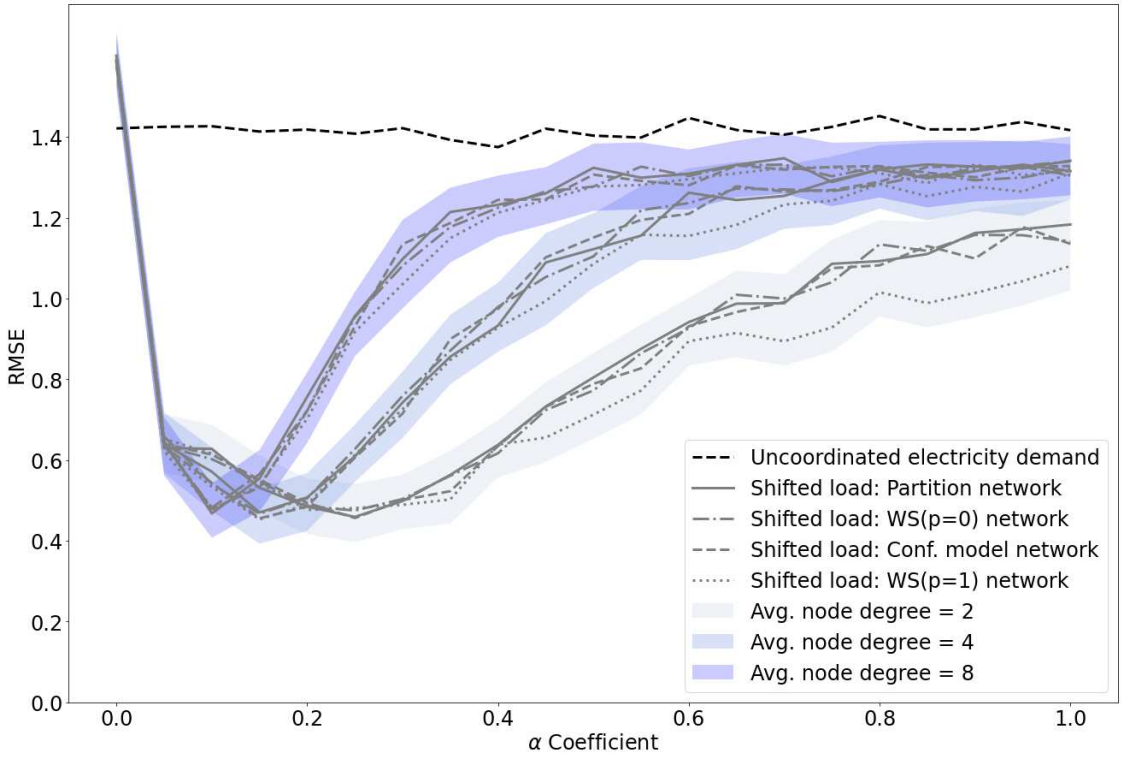

Figure 2. Impact of network topology on peak control and reduction illustrated for a 6 hour time shifting window selected due to Group 1 results (§2.2.1). The RMSE (root mean square error) values show the deviation from a flat (average) demand profile, with zero being totally peak-free. Each network average degrees cluster comprises of shifted demands for the following four networks: partition, ring lattice (WS(p=0)), random config. model and random (WS(p=1)). FHWM bandwidth for node degrees 2, 4 and 8 are 0.58, 0.4 and 0.24 correspondingly.FHWM bandwidth for node degrees 8 and 10 are virtually identical and hence only 8 is shown. Note that RMSE values for networks with node degree greater than 8 increase at approximately the same rate as the ones for networks with node degree of 8.

range of the load redistribution limit α for networks with node degrees 2–4, but its effectiveness is limited to a very narrow range of α values with higher node degrees.

The overall impact of these results on peak demand reduction is significant. An analysis of all implemented scenarios shows that the largest reduction of peaks in electricity consumption (average 59%, standard deviation 13% and maximum of 73%) can be achieved in the networks of node degree 4 and with α values ranging between 5% to 25%. The reduction of peaks regardless of the choice of α, on average, is 31% with standard deviation 21%. While this striking difference highlights the utility of choosing an optimal value for the load redistribution limit α, it also demonstrates that significant reductions can be robustly obtained across a wide range of chosen values for α.

3. Extension of load coordination schema for thermal loads

Loads from heating and cooling systems are not only significantly larger than those from a typical large home appliance modelled above, they are also time constrained through a combination of weather and lifestyle and hence known to have a significant impact on network peaks. The overall success of a peak coordination schema, such as that described here, will therefore largely depend on its ability to manage such loads. Hence, we now investigate the impact of extending the ABM to include such large time-constrained loads.

To run the extended ABM model, we choose the scenario group with optimised parameters (time window of 6h and network average degree of 4) that, in our previous experiments in §2.2.1 and §2.2.2, guaranteed the greatest peak demand flattening results (Table 2). We also expect that the time shifting window for our heating loads will, in practice, be considerably smaller due to the lower flexibility in how much they can be shifted compared to the loads considered earlier. For example, there would be little use in supplying heat to a home six hours after it is usually needed, as is the case with our most optimal result in §2.2.1. On the other

hand, we can expect predictably stable demand during summers in cooling dominated climates and winters in heating dominated climates, allowing thermal loads to be brought forward in addition to being delayed. Hence, we constrain the time shifting windows for our heating loads to either one or two hours either side of "scheduled" demand. In other words, the total window for heating operation is increased by two hours (split one hour each side of scheduled demand) or four hours (split two hours each side). Hence, the extended model is purposely loaded against peak flattening through the use of significantly larger loads that are also highly constrained in how much they can be shifted, but counterbalanced by the choice of the most optimal scenario group from the previous results. It is noteworthy that while the need to know heating or cooling schedules increases the information needed to implement our system, it is a quantity readily obtained from a modern domestic controller.

Our extended model achieves the greatest peak electricity demand flattening when the load redistribution limit $\alpha \approx 10\%$ and the time shifting window for heating loads is equal to 4 hours. Figure 3 illustrates the typical load profile of a network with three neighbours with uncoordinated and coordinated loads. Our findings show that while a two-hour time window of shifting heating operation results in a maximum 44% of peak flattening (mean 21%, s.d. 14%), a four-hour time window in a maximum 61% reduction (mean 33%, s.d. 23%), consistent with the idea that greater flexibility would result in greater flattening. Note that the minimum reduction for both scenarios is zero. Furthermore, the analysis of maximum ramp rates (kW/half hour) shows that reductions of 31% and 29% can be achieved for four-hour and two-hour time windows correspondingly. These results, though lower than for non-thermal loads, show substantial reductions and are consistent with the findings presented earlier.

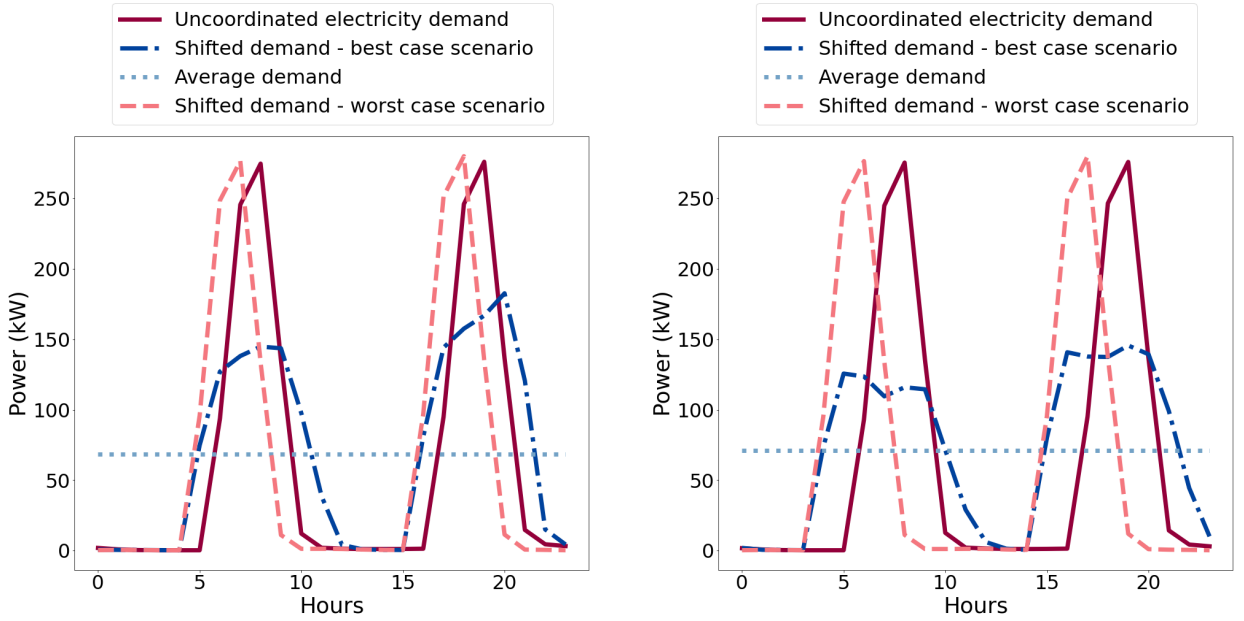

(a) 2-hour heating load shifting time window (1h on either side of scheduled demand).

(b) 4-hour heating load shifting time window (2h on either side of scheduled demand).

Figure 3. Hourly load profile of a simple network with just three neighbours comparing coordinated demand (best and worst cases) against constant average and uncoordinated demand for two-hour and four-hour heating load shifting windows.

3.1. Analysis of heating operation schedules

Since thermal energy demand drives indoor comfort, and our extended ABM will unpredictably interrupt the operation of the heating or cooling system, it is necessary to investigate the extent of disruption to the heating schedule imposed by our new extended model. We do this by analysing the distribution of run-lengths of heating operation outage hours for each dwelling in the network. That is, how long, on average and maximum, does a typical home experience an interruption in heating during the morning or evening period? The normalised distribution of run-lengths of outages for both the two-hour and four-hour time

window scenarios in Figure 4 suggests that the most common heating outage length is 15 minutes for the two-hour window, while it is 105 minutes for the four-hour window. This is due to the fact that the system is able to advantageously use the larger window of four hours to simply shift longer heating periods, whereas it is "forced" to break this schedule up into smaller chunks in the two-hour window. Longer breaks are also evident in the two-hour window, but are significantly less likely to occur. Further analysis shows that, on average, a single building is expected to have two outage events per day for the four-hour shifting window, with an average event length of 66 minutes, standard deviation of 42 minutes and total outage length of 162 minutes. For the two-hour shifting window, we observe an average of three outages per day with an average event length of 38 minutes, standard deviation of 23 minutes and a total outage length of 120 minutes.

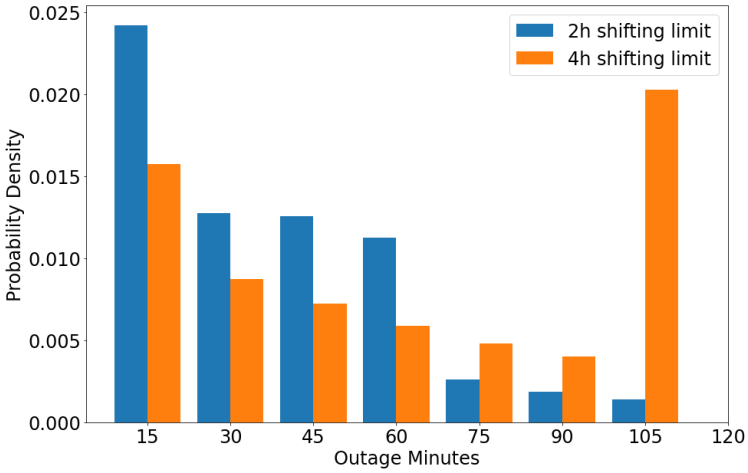

Figure 4. Normalised distribution of run-length of heating operation outage hours for two-hour and four-hour heating load shifting time window.

4. Discussion

Our main results are that interactions between only small numbers of buildings are needed to achieve significant peak-load reductions, that these are mostly independent of network topology and that they are robust over a wide range of other key parameters. These new insights are also interesting from the perspective of complexity and network science, as they reinforce findings in other application areas that the theoretically optimal size for coordination in networks can be surprisingly small, such as models of flocks of birds and firefly synchronisation. The greatest peak demand flattening occurs when the time shifting window is equal to six hours, the network degree (i.e., number of neighbours) is four buildings and the load redistribution limit α is between 10% and 25% of the neighbourhood's peak load. When $\alpha = 1$ or $\alpha = 0$ no peak reduction is seen in the network. This is similar to game theoretic approaches—used to study the formation of networks—which conclude that, if agents can observe each other's actions and outcomes over time and all agents have the same preferences and face the same form of uncertainty, then they develop similar payoffs over time [51]. However, we find that even a poor choice of α, on average, results in a 31% reduction in peak demand. Hence, the range of possible reductions predicted by our approach (31% to 73%) are far greater than even the predicted range of reductions in the DSM literature of between 13% to 50%.

Figure 5 illustrates the typical load profile of a network with just three neighbours with uncoordinated (i.e. occurring near-simultaneously) and coordinated loads, the latter for both highly optimised (best case) and non-optimised (worst case) parameters. The effect on ramp rates is also dramatic. That is, for the best case peak reduction scenario (i.e. $\alpha = 0.15$ the maximum ramp rate (kW/half hour) of schema-coordinated load can be reduced by 65% of the maximum ramp rate of the original, uncoordinated, load. In contrast for the worst case scenario when $\alpha = 0.95$, the maximum ramp rate of schema-coordinated load is 8% higher than the maximum ramp rate of the original uncoordinated load. Strikingly, our results demonstrate that network topology does not significantly influence peak flattening. This suggests that it is the simple presence of connections between dwellings that is important, rather than the manner of connection. However, there is a limit to the utility of the number of connections, or average degree of the network. Not only does

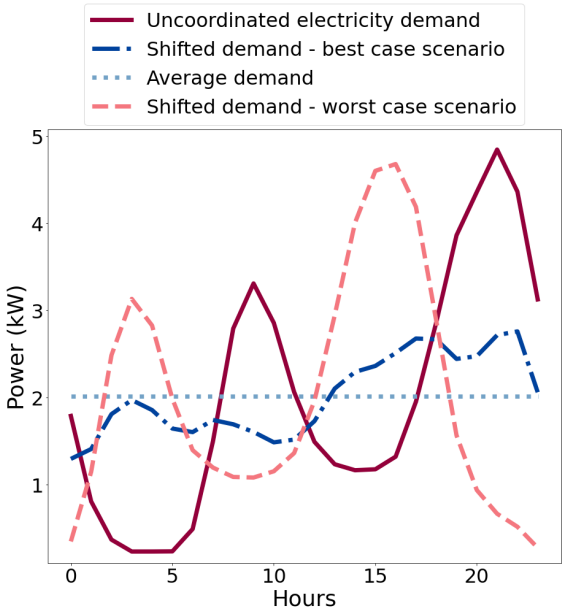

Figure 5. Daily typical total load profiles of a network with just three connected neighbours, comparing coordinated demand (best and worst cases) against constant average and uncoordinated demand.

increasing the average degree not improve the effectiveness of the peak coordination strategy, but it also limits the effective range of α to a very small window. This is analogous to the social behaviour of animals where it has been observed that, due to homogeneous interaction, animal social contact networks are not scale-free (i.e., node degrees do not follow power-law degree distribution) [52]. A second notable similarity with models of biological systems—such as flocking birds—is that the optimal number of neighbours is small. For example, birds are known to interact with a small number (six to seven) of neighbours to form a flock ([42], [39]).

The impact of the window within which behaviours can be shifted is observed to be optimal at 6 hours (RMSE = 0.46), though substantial reductions in peak demand can also be observed at the other intervals, with the 12-hour window being the "worst". In this case an RMSE of 0.65 is obtained, i.e., 19% worse than the 6-hour window, but still 54% better than with no coordination (RMSE = 1.42). It is noteworthy that the time window only specifies the range within which an energy consuming action can be deferred. In our modelling, agents randomly distribute loads within this window, which is consistent with the behaviour of an unmediated (i.e., automatic) controller. To what extent such behaviour can be expected from human-mediated action, were such mediation deemed useful, remains to be seen.

Given that thermal loads, such as those from a heating or cooling system, tend to be large in absolute terms and the key driver of peak loads, it is pertinent to ask whether such loads can be deferred for 3 to 12 hours. After all, the impulse to use heating and cooling is strongly dependent on external weather conditions, and there may be little flexibility in the timing of these loads. However, unlike some appliances, such as some washing machines whose individual cycles may be hard to interrupt once started, heating and cooling systems are fundamentally *interruptible*. Hence, it is possible, in principle, for a heating or cooling system to temporarily interrupt operation, with the possibility of restarting in the next 15 minute interval. This is entirely within the remit of the schema propose here since there is no decision memory – the system makes decisions independent of those made in previous intervals. Our tests of such loads using smaller shifting windows of only two or four hours demonstrate the striking possibility that even with the flexibility of just an hour before or after scheduled demand in the timing of these loads, it is possible to obtain a 44% reduction in peak load demand. This widens to 61% in a $\pm$2-hour window; both results being the maximum expected savings. These reductions are associated with a 29% and 31% reduction in ramp rates for the two-hour and four-hour cases, respectively (e.g., see Figure 6); and an average outage length of 38 and 66 minutes respectively. The standard deviation for outage lengths for the four-hour case (42 minutes) is almost two times higher than for the two-hour case (23 minutes), indicating that households across the

sample experience much higher variability of outage lengths as the time window increases.

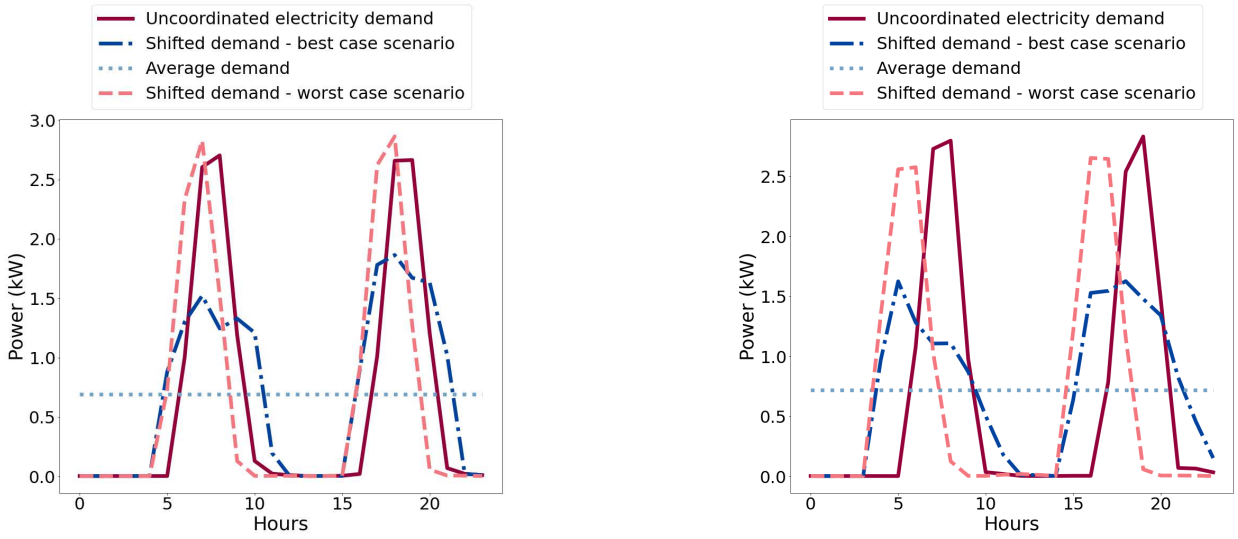

(a) 1-hour heating load shifting time window.

(b) 2-hour heating load shifting time window.

Figure 6. 24-hour load profiles of a random dwelling for 2-hour (a) and 4-hour (b) load shifting time windows. Each graph shows: the peak load coordination schema achieving the most peak demand flattening, the peak load coordination schema achieving the least peak demand flattening, the profiles when no peak coordination schema is applied and constant average demand.

Naturally, the drift in indoor temperature caused by a cessation of the heating or cooling system is strongly dependent on the thermal characteristics of the building envelope itself. Highly inefficient envelopes will cause a rapid drift away from comfortable temperatures, resulting in high ramp rates on the network when the system is switched back on. Conversely, well insulated or thermally heavy constructions will result in smaller network ramps. A second factor that can significantly influence this performance is the definition of thermal comfort itself. It is obvious that a narrow definition of comfort, e.g. within a $\pm$2K tolerance as defined in the international ISO 7730 standard [53], would result in more rapid excursions of indoor temperatures beyond comfortable levels, during periods of drift. The wider the definition, as for example suggested in recent research [54] or as adopted in countries such as India [55], would result in greater flexibility, and hence fewer network peaks. The influence of both these factors merits further investigation.

In summary, we show that significant reductions in peak loads are achievable through building-to-building load coordination within large networks. The theoretically optimal number of coordinating entities is surprisingly small and analogous to complex natural systems, whilst being network agnostic. These benefits are conferred in the presence of a very small information load at the level of an individual dwelling, i.e., the current load draw in the neighbourhood and the maximum "allowed". This is in stark contrast to widely adopted DSM schemes that use optimisation techniques and are limited by their dependency on the availability of historical data and forecasts [56, 57]. In the future, such coordination will no doubt become essential to manage the huge shifts currently underway in both the supply and demand side of the global energy system, i.e., increasing use of intermittent renewable generation and electricity as the only fuel for cars, space heating and space cooling.

5. Methods

In this section we describe in detail the methodology used for the numerical results described in previous sections. First, the different network topologies that were investigated are detailed. Next, we consider possible modelling approaches to investigate the problem that can adequately represent our load sharing schema. Finally, we describe our model set-up and the peak coordination algorithm and underlying data assumptions.

5.1. Network topologies

There are a wide range of network topologies described in the literature, of which *partition* and *small-world* topologies (defined in subsections 5.1.1 and 5.1.3) cover all the essential features of real world energy system networks, and hence are commonly used for modelling smart grid communication and control networks [58]. These can be benchmarked against *random* networks that have no inherent clustering into groups. Hence, numerical experiments were run using these three network topologies, across a range of network parameters, in order to compare and assess how they influence the effectiveness of a given control strategy. We ran simulated networks with 100 nodes – i.e. 100 dwellings – as a conveniently large number sufficient to contain several groups of neighbours and broadly representative of real networks. For example, the median number of consumers per substation on low voltage electricity distribution systems is approximately 100 [38]. The two essential features of any network are its *nodes* and *links* (or edges). In the following description *nodes* refer to the dwellings and *links/edges* to the connections between them.

5.1.1. Random Networks and the Configuration Model

Random networks are most commonly generated using Erdős and Renyi's (ER) random graph model [59]. This is a network with n nodes, where each node is linked to another (its *neighbour*) with probability $0 \leq q \leq 1$. This parameter controls both the density of the network as well as the *degree* of the nodes, defined as the (average) number of links per node. Figures 7a–7b illustrate how the value of the probability q can affect the structure of random networks.

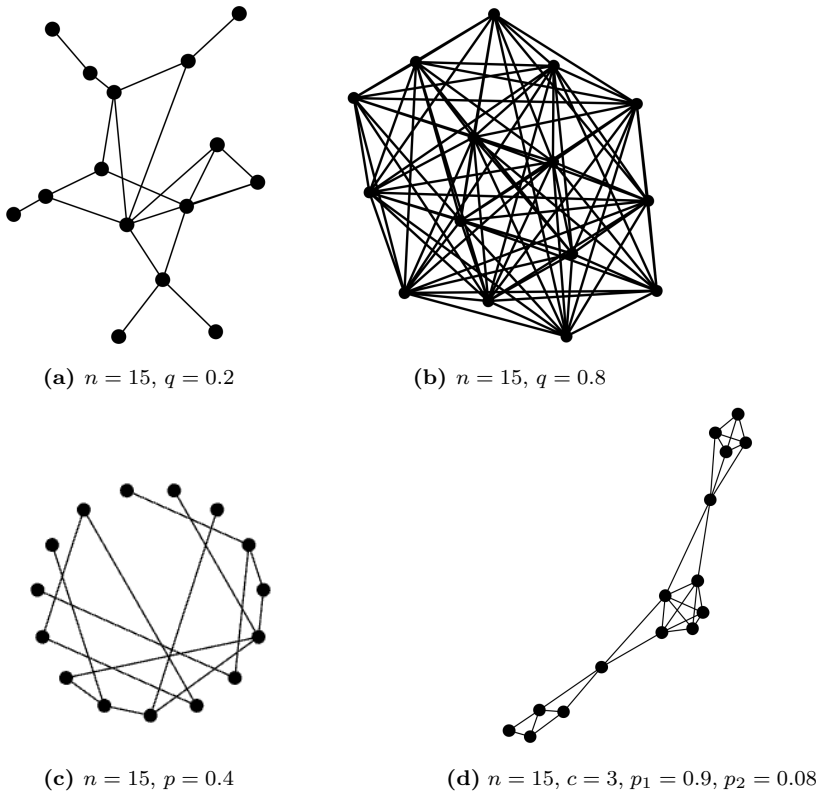

(a) $n = 15$, $q = 0.2$ **(b)** $n = 15$, $q = 0.8$

(c) $n = 15$, $p = 0.4$ **(d)** $n = 15$, $c = 3$, $p_1 = 0.9$, $p_2 = 0.08$

Figure 7. Different network topologies, showing (a) & (b) examples of random networks for different choice of link probabilities q, (c) a partition network that has intra- and inter-group connection and (d) a Watts–Strogatz *small world* network with local connections and long-range short-cuts.

However, ER networks lack certain important characteristics such as the ability to specify the precise degree for a given node [60], which is important to carefully control to ensure results are comparable. This aspect of random graph models can be improved by using the configuration model, in which the degrees of nodes are prescribed beforehand. [61–63].

5.1.2. Small world Networks

Small world networks, generated by the model of Watts and Strogatz (WS), can be used to represent the characteristics of real-world networks with a small number of links connecting any pair of nodes [64]. A small world network of n nodes is generated by the following algorithm [64]:

(i) generate a grid with n nodes such that the nodes can be arranged in a regular lattice or ring;

(ii) connect each node in the ring to its k nearest neighbours (where k is an even number for symmetry);

(iii) "rewire" each link in the regular network with probability p – i.e., disconnect it from one of its neighbours and connect it with another node that is chosen uniformly at random from the other nodes (often using pairwise swapping to preserve the degree of each node).

Figure 7c illustrates a small world network of $n = 15$ nodes, where number of nearest neighbours $k = 2$ and probability of rewiring a link is $p = 0.4$. When the rewiring probability $p = 0$ the network remains a regular lattice with high local clustering [65] but as rewiring probability increases to $p = 1$ the small world network is the same as a random network [63] with no local structure. Hence WS networks can be used to represent a spectrum of network topologies between these two extremes, with a range of local connectivity.

5.1.3. Partition Networks

The connectivity of the networks into local groups can be further controlled using the partition network model, which separates nodes into different communities. Two nodes in the same community form a link with probability $0 < p_1 \leq 1$ and nodes of different communities are connected with probability $0 \leq p_2 < 1$, with $p_1 > p_2$ for distinct communities to exist. Figure 7d illustrates a typical partition network with a constant degree $k = 4$.

5.2. Modelling approach

There are two alternative design approaches available for modelling complex systems: top-down and bottom-up. The top-down approach starts with specifying system parameters and outcomes at the macro-scale and often assumes global knowledge of the system. These are then passed down the modelling chain to generate a system response. In the bottom-up approach, the system is designed by specifying the requirements and capabilities of individual components, with the global behaviour expected to emerge out of interactions between the components and their environment [66]. In a situation when the global state of the system is unknown, interactions between components are complex and there is a lack of data, the bottom-up approach is better suited. It is obvious that the simple schema we described in Section 2.1 requires a bottom-up approach, particularly as it involves no centralised control.

Given that we are interested in the behaviour emergent through the interaction of agents (buildings or dwellings) within a system that are capable of taking actions in relation to their local environment (network neighbourhood), we use the well-known agent based modelling (ABM) bottom-up modelling framework. As it is probabilistic in nature, it can incorporate the high levels of uncertainty that are present in modelling social phenomena and allows the study of interactions between components and/or their emergent collective behaviour ([67]; [68], [69]). The main advantage of ABM over other modelling techniques (e.g., stochastic modelling or optimisation) is its ability to discover emergent properties.

Indeed, since energy systems are considered complex dynamical networks with multiple components that interact, adapt and evolve [70], several studies have employed ABMs to study energy infrastructure and electricity markets [71–73], including several DSM strategies. Peak demand reductions envisaged by these DSM studies range between 9% and 17% [26, 74–78] though none, as discussed, consider peak coordination between neighbours.

5.2.1. ABM Model for coordinating peak time electricity demand

Here we describe the ABM employed to investigate the system-level emergent result of scheduling of various shiftable appliances in different networks of dwellings for the purpose of optimal peak coordination. The effect of three key aspects on peak reduction were investigated, based on §5.1 and §2.1: (i) the effect of network topology, including both the network structure type and the average number of neighbours; (ii) the

length of the time window within which a given agent is allowed to shift demand and (iii) the amount of load allowed to be shifted by any single agent, as proportion α of the peak neighbourhood load l_{max}. Hence, these are carefully controlled within our model.

Each dwelling in the network is considered an agent with defined properties, as shown in Figure 8. The ABM simulation consists of the following steps. The model is calibrated using input data, with constraints and rules defined in the load coordination schema in §2.1. The system is then simulated for a period of one week[1], updating usage through a decision cycle every 15 minutes – an interval often used for real-time physical modelling of electricity networks and analysing peak load behaviour [79–81]. The choice of these time-frames is unlikely to affect our results given that either being longer or shorter merely affects the total number of observations, but not the nature of the decisions, which is the central aspect of this model.

Thus, after initialisation of the agents (Fig. 8(a)) and the network environment (Fig. 8(b)), the ABM runs in a cycle that can be described in three stages (Figure 8(c)): 1. agents observing their neighbourhoods; 2. agents making decisions; and 3. agents updating their inner state and behaviour.The agents observe their neighbourhood's overall usage over the last 15 minutes but do not influence each others decisions directly. A simple controller in each dwelling can then use this information to make decisions which affect the output of the model (Fig. 8(d)).

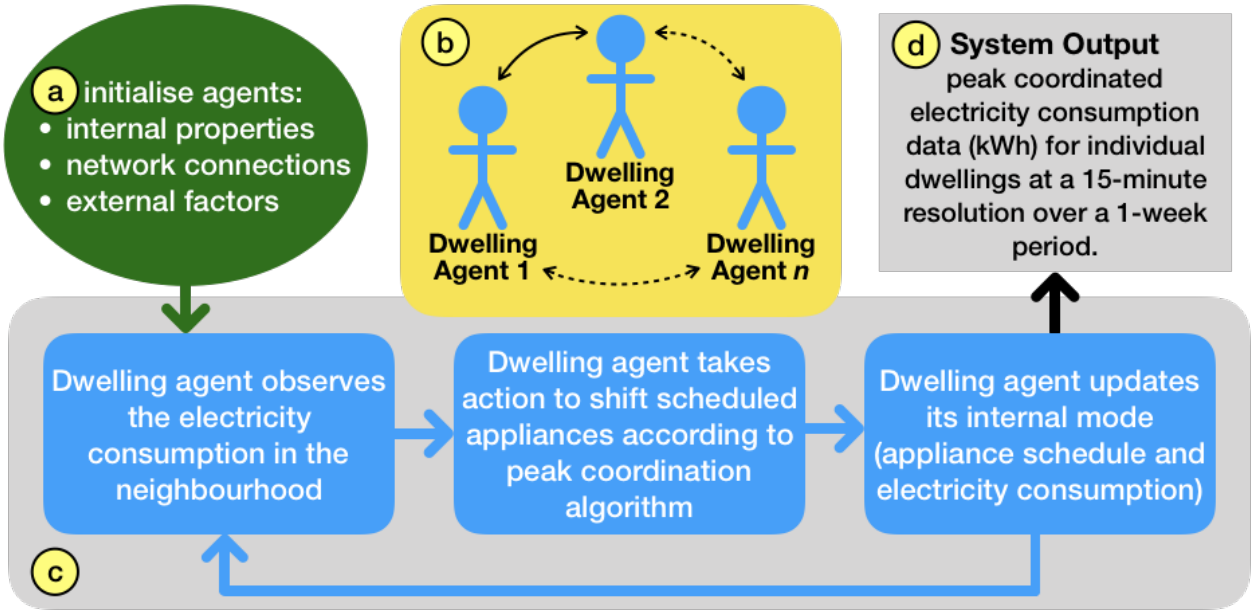

Figure 8. Agent Based Model (ABM) framework, showing Agent initialisation parameters (a), set up of the network of links between agents (b), the demand shifting routine (c) and system-level output (d).

The ABM is stochastic in nature in order to model a variety of household typologies and different behaviour patterns, hence multiple runs allow the variability in the model to be captured [82]. Initial trials of 30, 50 and 150 runs of the ABM demonstrated that data variability plateaued at around 30 runs. Hence the model was run 30 times for each scenario and the outcomes of these ensemble runs were averaged.

5.3. Model Set-Up

The scenarios implemented in the ABM model were arranged into two groups to analyse the system parametrically, one with each node having a fixed number of directly linked neighbours (average node degree) but variable time windows for demand shifting and the other with a range of degrees but fixed time shifting window, as shown in Table 1.

[1]This study does not consider seasonal variation of electricity demand hence, for simplicity, a single week is considered throughout this work.

Scenario Group	Network Topology	Average degree	load redistribution limit interval	Time window
Group 1	variable	4 (fixed)	$0 \leq \alpha \leq 1$	3h, 6h, 12h
Group 2	variable	2, 4, 8, 10	$0 \leq \alpha \leq 1$	3h (fixed)

Table 1. Scenario structure for two groups of ABM simulations. Group 1 consists of $4 \times 1 \times 21 \times 3 = 252$ scenarios, and Group 2 consists of $4 \times 4 \times 21 \times 1 = 336$ scenarios. Network topologies varied between: partition, ring lattice (WS($p = 0$)), random using the small world scheme WS($p = 1$)) and the configuration model with fixed node degree (see Table 3 for details). The average degree is the number of directly connected neighbours in the network. α is the load redistribution limit (Sec. 5.4) increased at intervals of 0.05 over the indicated range. Time window is the maximum interval of time that a load can be shifted within, with the actual length of shift being randomly determined.

In preliminary runs, windows of 15 and 30 minutes were also tested but the outcomes did not show any significant reduction of peaks from that when no schema was applied.

For thermally constrained loads, using the extended ABM model, the previously identified optimised parameters used are shown in Table 2.

Network Topology	load redistribution limit interval	Time window (shiftable loads)	Time window (heating loads)
CM($d = 4$) (See Table 3)	$0 \leq \alpha \leq 1$	6h	2h (1 + 1), 4h (2 + 2)

Table 2. Scenario group parameters for extended ABM simulations.

5.3.1. Network Initialisation

The following network topologies were generated using Python library NetworkX [83] and Java library jGraphT [84]: partition networks with probability of links within communities $p_1 = 1$ and probability of links between communities $p_2 = 0$, representing disconnected neighbourhoods which are each internally fully connected; small world networks with a rewiring probability $p = 0$ – WS($p = 0$), i.e., simple ring lattices with various degrees representing a system of connected neighbourhoods; small world networks with rewiring probability $p = 1$ – WS($p = 1$), i.e., random networks with no community structure; configuration model networks with each node having pre-determined degree $d = 2$, $d = 4$ or $d = 8$ – CM($d = 2$), CM($d = 2$) and CM($d = 8$), giving random networks with fixed (rather than distributed) degrees. See Table 3 for detailed statistics of the networks[2].

5.3.2. Model initialisation

The ABM for peak coordination and reduction was implemented using the open source RePast Simphony agent based modelling environment in Java [85]. The system initialisation (Fig. 8a) includes:

(i) internal properties (described below);

(ii) network connections (Fig. 8b) – described in Section 5.1 and listed in Table 3;

(iii) external factors – system parameters including total system size, threshold (τ) for action, time-window for shifting of appliances and each agent's neighbourhood's maximum demand level (see §5.4).

Once the input data has been provided, the internal properties of the "dwelling" agents in the network are initialised. Each dwelling is assigned a set of loads representing appliances according to appliance ownership rates defined in [46]. For example, if the ownership rate for the appliance A is 80% then 80% of the dwellings will be selected randomly and the appliance A added to the list of appliances they own.

[2]Note that in order to generate network topologies with comparable average degrees, without loss of generality, a few Partition networks have 99 nodes.

Network Topology	Average Degree	Edges	Communities	Clustering Coefficient
Partition	1	50	50	0
Partition	2	99	33	1
WS($p = 0$)	2	100	–	0
WS($p = 1$)	2	100	–	0
CM($d = 2$)	2	100	–	0
Partition	4	200	20	1
WS($p = 0$)	4	200	–	0.5
WS($p = 1$)	4.06	201	–	0.03
CM($d = 4$)	4	200	–	0.02
Partition	8	396	11	1
WS($p = 0$)	8	400	–	0.64
WS($p = 1$)	8.06	400	–	0.06
CM($d = 8$)	8	400	–	0.05
Partition	10	495	9	1
WS($p = 0$)	10	500	–	0.66
WS($p = 1$)	10	500	–	0.09
CM($d = 10$)	10	500	–	0.08

Table 3. Networks statistics, showing different network generation models and parameters: defined degree d for the configuration model (CM); rewiring probability p for the small world (WS) networks; and number of communities for the Partition model. Also shown are some of the resulting measured topological features – average degree (number of links) and clustering coefficient (degree of *co-connectivity*).

To guarantee variable and realistic appliance usage schedules, initial appliance time schedules are generated from a truncated normal distribution, based on type of occupancy discussed in detail in §5.4.3. Afterwards, initial consumption patterns for appliances are generated for each dwelling agent, based on occupancy types and statistics such as occupant activity/inactivity times. The last step of the initialisation is to define the network of interactions between dwellings, based on the types given in §5.3.1.

5.4. Peak coordination algorithm

After initialisation of the model parameters, initial load demands (§5.3.2 & Fig. 8a) and network topology (§5.1 & Fig.8b) the peak coordination algorithm is initiated, based on the actions set out in Section 2.1. The aim of the algorithm is to determine the action to be taken at the next time-step t, based on the previous state at the preceding 15-minute interval $t - 1$.

For each time-step t, the model updates the properties and behaviour of every agent and obtains the sum of each agent's neighbours' electricity demand at time $t - 1$. The neighbourhood peak load, l_{max} is modelled by summing the peak loads that would occur within an agent's *closed* neighbourhood (that of itself *and* its network neighbours) over an arbitrarily chosen one week time-scale without the peak coordination algorithm. This simulates the situation where a period from the previous system history would be used to estimate l_{max}. A threshold is then calculated by multiplying l_{max} by a scaling factor α. The parameter $\tau = \alpha \times l_{max}$ subsequently acts as a *load redistribution limit* and controls the total amount of load that can be shifted in each time-step. The case of $\alpha = 0$ corresponds to no load-shifting and is therefore reverts to the baseline-case, whereas $\alpha = 1$ allows agents the potential to simultaneously shift all load to the same time and hence cause a new peak where there was once a dip in demand. Next, the electricity consumption of each dwelling agent and its network neighbours at time $t - 1$ is compared with τ and one of two actions is taken, as follows. If electricity consumption in the closed neighbourhood is greater than or equal to τ, the decision to decrease electricity demand at time step t will be made and a load that can be shifted will be identified from the appliance list. The load is then shifted to a *demand pool*, to be rescheduled within the defined shifting time window N. Otherwise, if the electricity consumption of the dwelling is below τ the decision to increase electricity demand at time step t will be made and an appliance-load within the demand pool will be identified. The electricity demand for the agent will then be updated for that time step. The simulation then outputs the computed electricity loads for each dwelling in 15 minute intervals over one

455 week. This process is then repeated for each 15-minute interval for the whole computed week. The total
456 number of steps over one week is hence 672.

457 *5.4.1. Algorithm details*

The algorithm below illustrates the sequence of steps described above. Defining the set of all dwelling agent nodes $D = \{d_1, d_2, ..., d_n\}$, the undirected network of agents is denoted as a graph $G(D, C)$, connecting nodes D via links given by $C = \{(d_i, d_j)\}$ where $1 \leq [i, j] \leq n$ and $i \neq j$. The neighbourhood of agent d_i is given as:

$$N(d_i) = \{d_j \mid (d_i, d_j) \in C\}.$$

Further, the *closed* neighbourhood of d_i is defined as the set containing both d_i *and* its neighbourhood $N(d_i)$, given by the union $N[d_i] = d_i \cup N(d_i)$. The electricity consumption of an agent d_i at time step t is denoted $e(d_i, t)$, so the electricity consumption of agent d_i's *closed* neighbourhood at time t is thus given by:

$$E_{N[d_i]}(t) = \sum_{d_j \in N[d_i]} e(d_j, t).$$

Similarly, $\hat{e}(d_i)$ denotes the *sequence* of all demands for every 15 minute interval in $1 \leq t \leq 672$ for agent d_i over the whole week, and the sequence of electricity consumption values for d_i's closed neighbourhood is the sum over this and denoted $\hat{E}_{N[d_i]}$. Hence the peak electricity consumption of agent d_i's *closed* neighbourhood is defined as:

$$\text{Peak}_{N[d_i]} = \max_{1 \leq t \leq 672} \hat{E}_{N[d_i]}.$$

458 The algorithm 5.1 shows workflow of the ABM in detail.

Algorithm 5.1: Peak coordination algorithm

Data: set of Dwellings D; network topology of connections; base load profiles; occupancy type; list of appliances (A), their unshifted schedules, cycle length and mean electricity demand; α load redistribution limit for peak electricity consumption in neighbourhoods of agents $0 < \alpha \leq 1$

Result: electricity load (in kW) for individual dwellings in 15 minute intervals for a period of one week

```
Initialize dwellings with input data;
for each d_i in D do
    generate appliance consumption patterns.
for TimeStep = 1 : (24 * 4 * 7) do
    for each d_i in D do
        if E_{N[d_i]}(t − 1) ≥ α × Peak_{N[d_i]} then
            determine appliance(s) which can be delayed to trigger a
            decrease in electricity demand at time t
            if appliance(s) operation is time constrained then
                delay the load if and only if the time constraint
                is not violated.
        else
            determine appliance load(s) from the pool which can
            be shifted to be brought into use now to increase
            electricity demand at t to match the target α × Peak_{N[d_i]}.
            if appliance(s) operation is time constrained then
                shift the load if and only if the time constraint
                is not violated.
    for each A_k in A do
        if ScheduleStart(A_k) == TimeStep then
            Switch A_k on
        if switch off time then
            Switch A_k off
```

5.4.2. Base load Profiles

Base loads (often referred to as *static loads*) represent uncontrollable energy demand. These loads cannot be influenced by control systems and have no inherent flexibility (e.g. lighting, computers). Each agent in the network was initialised with an individual base load electricity demand. The generation of profiles for networks of 100 buildings was done using the "Artificial Load Profile Generator for DSM" (ALPG) tool [46]. This open source tool generates realistic, high resolution load profiles through simulation of occupant behaviour, validated against measurements obtained in a field-test [46]. The base load profiles are illustrated in Figures 9a and 9b.

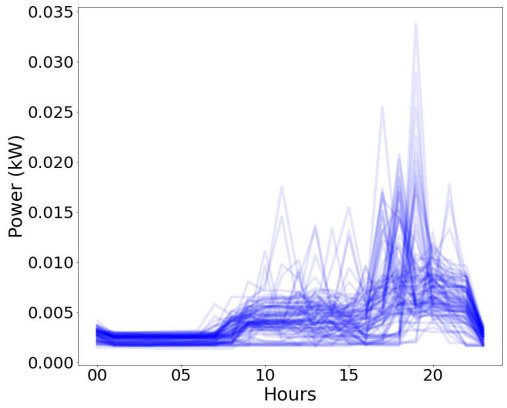

(a) Individual base load profiles on a typical day for the network of 100 agents.

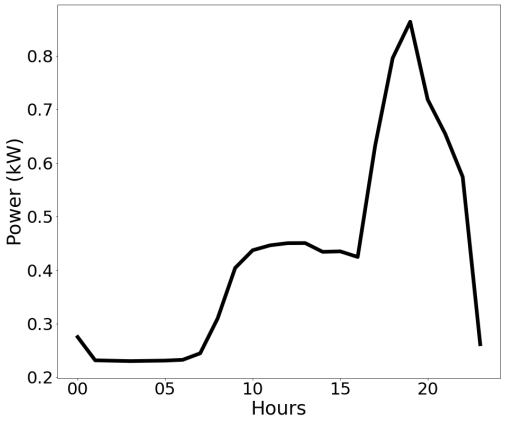

(b) Sum of base loads on a typical day for all agents in a network size of 100.

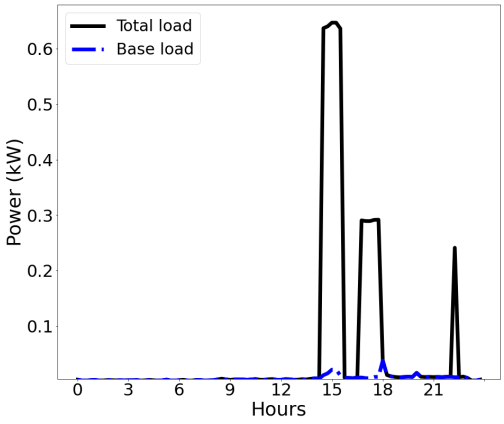

(c) Base and total load for a single, randomly selected, agent.

Figure 9. Example base load profiles over a single weekday for (a) 100 individual agents (b) total base load for all agents and (c) base and total load for a single, randomly selected, agent. Note that the base load, while small, compared to total load is in itself "peaky".

5.4.3. Occupancy Types and Schedules

There exist a wide variety of domestic occupancy types depending on the number of people in a household, their ages, employment status etc., [86]. For simplicity, we consider just two: "employed" and "unemployed" (in a 70:30 distribution ratio) as it provides the two extremes of "intermittent" and "permanent" occupancy, respectively. An advantage of this simplification is that it reflects the profiles used in the ALPG tool noted above. The main difference between the two occupancy types is that a dwelling with "employed" occupants will initially be scheduled to only use appliances in the mornings or in the evenings, whereas appliances are scheduled randomly throughout the day for "unemployed" occupants.

5.4.4. Model Constraints

Since the focus of this paper is to investigate the impact of the network topology and average number of neighbours on the peak coordination schema it was assumed that all shiftable appliances can be shifted by the peak coordination algorithm (see §5.1), so factors such as appliance priority or appliance run-time factor (the ratio of time for which a particular appliance was in the running state during the previous time slot) are not included in the current scheme. However, given that thermal loads are usually the single largest load type, and their demand is time-constrained, we investigate them separately, see below.

5.4.5. *Thermal loads*

Loads from heating and cooling systems in buildings can be large. For example, a gas boiler or electric heat pump has a rated capacity about five times that of a typical large home appliance such as a dryer; and a domestic air-conditioning unit about twice as large as a typical appliance. Such loads are known to have a significant impact on network peaks [87]. This is due to both the size of the loads and their constrained timing. Unlike other loads which we have previously taken to be largely unconstrained, thermal loads usually operate in discrete intervals related to the need for the load – arising from a combination of weather and lifestyle. In the UK, for example, a pattern of heating once in the morning and once in the evening is common, with the typical length of each heating event varying between 2–3 hours [88]. For convenience and simplicity, we use the typical heating pattern in the UK as an embodiment typical of thermal loads and assume that (i) all the dwellings in the network will have a heating operation twice a day (ii) the length of each heating event is fixed and equal to 2.5 hours and (iii) the typical power rating for heating load is 12 kW, a sufficiently large capacity for most common heating loads, including heat pumps [89, 90]. To ensure variability and simulate the well-known "demand diversity factor", a heating schedule is generated for each dwelling in the network by randomly sampling within fixed intervals in morning (05:00–08:00) and in the evening (17:00–19:00).

Figure 10 illustrates the base and total load for a single, randomly selected, dwelling in our simulation. Compared to the load produced by the simple ABM model presented in Section 5 with no heating system included (Fig. 9) the total load when a heating system is included is significantly higher, as expected.

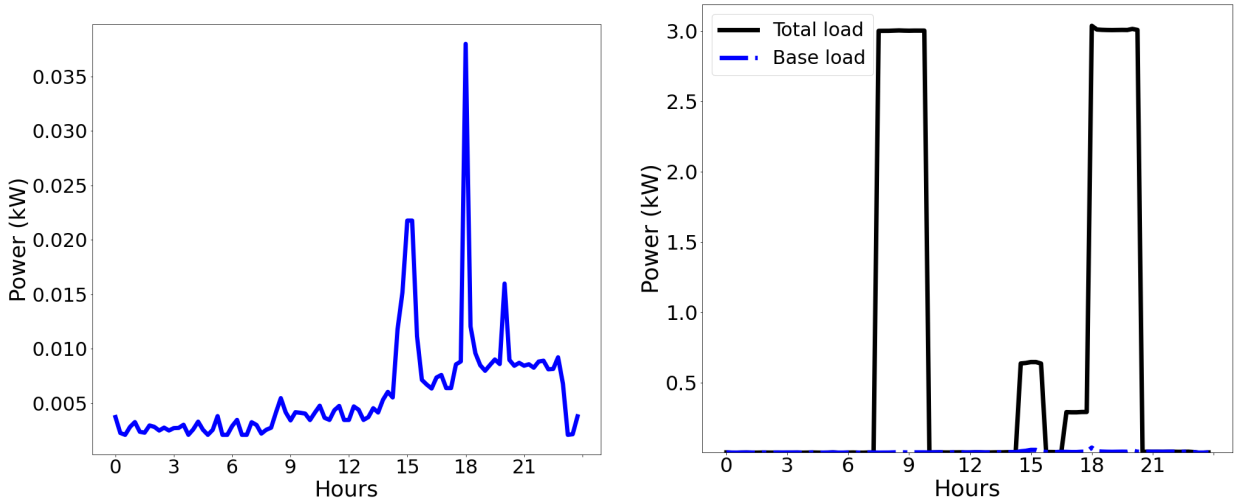

(a) Daily individual base load profile.

(b) Total and base load profiles.

Figure 10. Example base and base + total load profiles for a single, randomly selected, dwelling on a typical weekday. The large 3kW peaks are from the heating system, whereas the smaller peaks are from other appliances, per Figure 9c.

Data Availability

The data and codes that support the findings of this study are available from the following source:
`https://bitbucket.org/apoghosyan/zedipeaksupression/src/master/`

Author Contributions

All authors conceived the presented idea and planned the experiments. S.N. and N.M. provided technical lead. A.P. designed and implemented the agent-based model, carried out simulations and analysed the data. All authors contributed to writing the final version of the manuscript. All authors provided critical feedback and helped shape the research, analysis and manuscript.

Funding

This work was funded by the UK Engineering and Physical Sciences Research Council (EPSRC) grant EP/R008612/1 for the project "Zero Peak Energy Building Design for India (ZED-i)".

References

[1] Xiaodong Cao, Xilei Dai, and Junjie Liu. "Building energy-consumption status worldwide and the state-of-the-art technologies for zero-energy buildings during the past decade". In: *Energy and Buildings* 128 (2016), pp. 198 –213. ISSN: 0378-7788. DOI: https://doi.org/10.1016/j.enbuild.2016.06.089.

[2] Diana Ürge Vorsatz et al. "Heating and cooling energy trends and drivers in buildings". In: *Renewable and Sustainable Energy Reviews* 41 (2015), pp. 85 –98. ISSN: 1364-0321. DOI: https://doi.org/10.1016/j.rser.2014.08.039.

[3] International Energy Agency. *Tracking Buildings 2020*. https://www.iea.org/reports/tracking-buildings-2020. [Online; accessed 2021-13-05]. 2020.

[4] Abdeen Mustafa Omer. "Energy use and environmental impacts: A general review". In: *Journal of Renewable and Sustainable Energy* 1.5 (2009), p. 053101. DOI: 10.1063/1.3220701. URL: https://doi.org/10.1063/1.3220701.

[5] Nan Zhou et al. "Scenarios of energy efficiency and CO 2 emissions reduction potential in the buildings sector in China to year 2050". In: *Nature Energy* 3.11 (2018), pp. 978–984.

[6] Amos Kalua. "Urban Residential Building Energy Consumption by End-Use in Malawi". In: *Buildings* 10.2 (2020). ISSN: 2075-5309. DOI: 10.3390/buildings10020031. URL: https://www.mdpi.com/2075-5309/10/2/31.

[7] M. Piette and Sila Kiliccote. "Demand Responsive and Energy Efficient Control Technologies and-Strategies in Commercial Buildings". In: (Sept. 2006). DOI: 10.2172/901231.

[8] Miimu Airaksinen and Mika Vuolle. "Heating Energy and Peak-Power Demand in a Standard and Low Energy Building". In: *Energies* 6 (Jan. 2013), pp. 235–250. DOI: 10.3390/en6010235.

[9] M. Thyholt and A.G. Hestnes. "Heat supply to low-energy buildings in district heating areas: Analyses of CO2 emissions and electricity supply security". In: *Energy and Buildings* 40 (Dec. 2008), pp. 131–139. DOI: 10.1016/j.enbuild.2007.01.016.

[10] Joshua W. Busby et al. "Cascading risks: Understanding the 2021 winter blackout in Texas". In: *Energy Research Social Science* 77 (2021), p. 102106. ISSN: 2214-6296. DOI: https://doi.org/10.1016/j.erss.2021.102106. URL: https://www.sciencedirect.com/science/article/pii/S2214629621001997.

[11] Frances Ruth Wood et al. "The impacts of climate change on UK energy demand". In: *Infrastructure Asset Management* 2.3 (2015), pp. 107–119. DOI: 10.1680/jinam.14.00039. URL: https://www.icevirtuallibrary.com/doi/abs/10.1680/jinam.14.00039.

[12] Gertrud Hatvani-Kovacs et al. "Assessment of Heatwave Impacts". In: *Procedia Engineering* 169 (2016). Fourth International Conference on Countermeasures to Urban Heat Island, 30-31 May and 1 June 2016, pp. 316–323. ISSN: 1877-7058. DOI: https://doi.org/10.1016/j.proeng.2016.10.039. URL: https://www.sciencedirect.com/science/article/pii/S1877705816332428.

[13] Norman L. Miller et al. "Climate, Extreme Heat, and Electricity Demand in California". In: *Journal of Applied Meteorology and Climatology* 47.6 (2008), pp. 1834 –1844. DOI: 10.1175/2007JAMC1480.1. URL: https://journals.ametsoc.org/view/journals/apme/47/6/2007jamc1480.1.xml.

[14] Juan Añel et al. "Impact of Cold Waves and Heat Waves on the Energy Production Sector". In: *Atmosphere* 8 (Oct. 2017), p. 209. DOI: 10.3390/atmos8110209.

[15] Maximilian Auffhammer, Patrick Baylis, and Catherine H. Hausman. "Climate change is projected to have severe impacts on the frequency and intensity of peak electricity demand across the United States". In: *Proceedings of the National Academy of Sciences* 114.8 (2017), pp. 1886–1891. DOI: 10.1073/pnas.1613193114.

[16] Luis Ortiz, Jorge Gonzalez, and Wuyin Lin. "Climate change impacts on peak building cooling energy demand in a coastal megacity". In: *Environmental Research Letters* 13 (Aug. 2018). DOI: 10.1088/1748-9326/aad8d0.

[17] "Climate change impacts on trends and extremes in future heating and cooling demands over Europe". In: *Energy and Buildings* 226 (2020), p. 110397. ISSN: 0378-7788. DOI: https://doi.org/10.1016/j.enbuild.2020.110397.

[18] Haojie Wang and Qingyan Chen. "Impact of climate change heating and cooling energy use in buildings in the United States". In: *Energy and Buildings* 82 (2014), pp. 428–436. ISSN: 0378-7788. DOI: https://doi.org/10.1016/j.enbuild.2014.07.034. URL: https://www.sciencedirect.com/science/article/pii/S0378778814005726.

[19] "Impacts of climate change on energy consumption and peak demand in buildings: A detailed regional approach". In: *Energy* 79 (2015), pp. 20–32. ISSN: 0360-5442. DOI: https://doi.org/10.1016/j.energy.2014.08.081. URL: https://www.sciencedirect.com/science/article/pii/S0360544214010469.

[20] Bo Shen et al. "Addressing Energy Demand through Demand Response. International Experiences and Practices". In: (). DOI: 10.2172/1212423. URL: https://www.osti.gov/biblio/1212423.

[21] L. Wang, C.W. Yu, and F.S. Wen. "Economic theory and the application of incentive contracts to procure operating reserves". In: *Electric Power Systems Research* 77.5 (2007), pp. 518–526. ISSN: 0378-7796. DOI: https://doi.org/10.1016/j.epsr.2006.05.004. URL: https://www.sciencedirect.com/science/article/pii/S0378779606001222.

[22] Imran Khan. "Importance of GHG emissions assessment in the electricity grid expansion towards a low-carbon future: A time-varying carbon intensity approach". In: *Journal of Cleaner Production* 196 (2018), pp. 1587–1599. ISSN: 0959-6526. DOI: https://doi.org/10.1016/j.jclepro.2018.06.162. URL: https://www.sciencedirect.com/science/article/pii/S0959652618318122.

[23] Dian ce Gao and Yongjun Sun. "A GA-based coordinated demand response control for building group level peak demand limiting with benefits to grid power balance". In: *Energy and Buildings* 110 (2016), pp. 31–40. ISSN: 0378-7788. DOI: https://doi.org/10.1016/j.enbuild.2015.10.039. URL: https://www.sciencedirect.com/science/article/pii/S0378778815303534.

[24] S. K. Nayak, N. C. Sahoo, and G. Panda. "Demand side management of residential loads in a smart grid using 2D particle swarm optimization technique". In: *2015 IEEE Power, Communication and Information Technology Conference (PCITC)*. 2015, pp. 201–206.

[25] N. Javaid et al. "Energy Efficient Integration of Renewable Energy Sources in the Smart Grid for Demand Side Management". In: *IEEE Access* 6 (2018), pp. 77077–77096.

[26] Sarvapali D. Ramchurn et al. "Agent-based Control for Decentralised Demand Side Management in the Smart Grid". In: *The 10th International Conference on Autonomous Agents and Multiagent Systems - Volume 1*. AAMAS '11. International Foundation for Autonomous Agents and Multiagent Systems, 2011, pp. 5–12.

[27] Jin-Ho Kim and Anastasia Shcherbakova. "Common failures of demand response". In: *Energy* 36 (Feb. 2011), pp. 873–880. DOI: 10.1016/j.energy.2010.12.027.

[28] Niamh O'Connell et al. "Benefits and challenges of electrical demand response: A critical review". In: *Renewable and Sustainable Energy Reviews* 39 (Nov. 2014), pp. 686–699. DOI: 10.1016/j.rser.2014.07.098.

[29] Ying Guo et al. "A Simulator for Self-Adaptive Energy Demand Management". In: *Proceedings of the 2008 Second IEEE International Conference on Self-Adaptive and Self-Organizing Systems*. SASO '08. IEEE Computer Society, 2008, pp. 64–73. ISBN: 978-0-7695-3404-6.

[30] Benjamin L. Ruddell, Francisco Salamanca Palou, and Alex Mahalov. "Reducing a semiarid city's peak electrical demand using distributed cold thermal energy storage". In: *Applied Energy* 134 (Dec. 2014), pp. 35–44.

[31] Elham Shirazi and Shahram Jadid. "Cost reduction and peak shaving through domestic load shifting and DERs". In: *Energy* 124.C (2017), pp. 146–159.

[32] Pei Huang et al. “A hierarchical coordinated demand response control for buildings with improved performances at building group”. In: *Applied Energy* 242 (2019), pp. 684–694. ISSN: 0306-2619. DOI: https://doi.org/10.1016/j.apenergy.2019.03.148. URL: https://www.sciencedirect.com/science/article/pii/S0306261919305574.

[33] Dian ce Gao and Yongjun Sun. “A GA-based coordinated demand response control for building group level peak demand limiting with benefits to grid power balance”. In: *Energy and Buildings* 110 (2016), pp. 31–40. ISSN: 0378-7788. DOI: https://doi.org/10.1016/j.enbuild.2015.10.039. URL: https://www.sciencedirect.com/science/article/pii/S0378778815303534.

[34] Pei Huang and Yongjun Sun. “A collaborative demand control of nearly zero energy buildings in response to dynamic pricing for performance improvements at cluster level”. In: *Energy* 174 (2019), pp. 911–921. ISSN: 0360-5442. DOI: https://doi.org/10.1016/j.energy.2019.02.192. URL: https://www.sciencedirect.com/science/article/pii/S0360544219304025.

[35] Y. Zhou et al. “Demand response control strategy of groups of central air-conditionings for power grid energy saving”. In: *2016 IEEE International Conference on Power and Renewable Energy (ICPRE)*. 2016, pp. 323–327. DOI: 10.1109/ICPRE.2016.7871225.

[36] Pei Huang et al. “A coordinated control to improve performance for a building cluster with energy storage, electric vehicles, and energy sharing considered”. In: *Applied Energy* 268 (2020), p. 114983. ISSN: 0306-2619. DOI: https://doi.org/10.1016/j.apenergy.2020.114983. URL: https://www.sciencedirect.com/science/article/pii/S0306261920304955.

[37] M W Krentel. “The Complexity of Optimization Problems”. In: *Proceedings of the Eighteenth Annual ACM Symposium on Theory of Computing*. STOC ’86. Berkeley, California, USA: Association for Computing Machinery, 1986, 69–76. ISBN: 0897911938. DOI: 10.1145/12130.12138. URL: https://doi.org/10.1145/12130.12138.

[38] Giuseppe Prettico et al. *Distribution System Operators Observatory - From European Electricity Distribution Systems to Representative Distribution Networks*. https://publications.jrc.ec.europa.eu/repository/bitstream/JRC101680/ldna27927enn.pdf. [Online; accessed 2019-11-05]. 2016.

[39] Craig W. Reynolds. “Flocks, Herds and Schools: A Distributed Behavioral Model”. In: *SIGGRAPH Comput. Graph.* 21.4 (Aug. 1987), pp. 25–34. ISSN: 0097-8930. DOI: 10.1145/37402.37406.

[40] Alessandro Attanasi et al. “Information transfer and behavioural inertia in starling flocks”. In: *Nature physics* 10 (Sept. 2014), pp. 615–698. DOI: 10.1038/nphys3035.

[41] Michele Ballerini et al. “Interaction ruling animal collective behavior depends on topological rather than metric distance: Evidence from a field study”. In: *Proceedings of the national academy of sciences* 105.4 (2008), pp. 1232–1237.

[42] M. Ballerini et al. “Interaction ruling animal collective behavior depends on topological rather than metric distance: Evidence from a field study”. In: *Proceedings of the National Academy of Sciences* 105.4 (2008), pp. 1232–1237. ISSN: 0027-8424. DOI: 10.1073/pnas.0711437105. eprint: https://www.pnas.org/content/105/4/1232.full.pdf.

[43] Mehdi Moussaïd, Dirk Helbing, and Guy Theraulaz. “How simple rules determine pedestrian behavior and crowd disasters”. In: *Proceedings of the National Academy of Sciences* 108.17 (2011), pp. 6884–6888. ISSN: 0027-8424. DOI: 10.1073/pnas.1016507108. eprint: https://www.pnas.org/content/108/17/6884.full.pdf. URL: https://www.pnas.org/content/108/17/6884.

[44] D. Burini, S. De Lillo, and L. Gibelli. “Collective learning modeling based on the kinetic theory of active particles”. In: *Physics of Life Reviews* 16 (2016), pp. 123–139. ISSN: 1571-0645. DOI: https://doi.org/10.1016/j.plrev.2015.10.008. URL: https://www.sciencedirect.com/science/article/pii/S1571064515001748.

[45] Yoshinobu Inada and Hideaki Takanobu. “Flight-Formation Control of Air Vehicles Based on Collective Motion Control of Organisms”. In: *IFAC Proceedings Volumes* 43.15 (2010). 18th IFAC Symposium on Automatic Control in Aerospace, pp. 386–391. ISSN: 1474-6670. DOI: https://doi.org/10.3182/20100906-5-JP-2022.00066. URL: https://www.sciencedirect.com/science/article/pii/S1474667015318711.

[46] Gerwin Hoogsteen et al. "Generation of flexible domestic load profiles to evaluate demand side management approaches". In: *2016 IEEE International Energy Conference (ENERGYCON)*. IEEE Power & Energy Society, Apr. 2016, p. 1279.

[47] Noah Pflugradt et al. "Analysing low-voltage grids using a behaviour based load profile generator". In: *Renewable Energy and Power Quality Journal* (Mar. 2013), pp. 361–365. DOI: 10.24084/repqj11.308.

[48] Likhwelihle Kaira, M. Nthontho, and Shahidullah Chowdhury. "Achieving demand side management with appliance controller devices". In: Sept. 2014, pp. 1–6. DOI: 10.1109/UPEC.2014.6934611.

[49] Kathryn B. Janda. "Buildings don't use energy: people do". In: *Architectural Science Review* 54.1 (2011), pp. 15–22. DOI: 10.3763/asre.2009.0050.

[50] Jenny Love et al. "The addition of heat pump electricity load profiles to GB electricity demand: Evidence from a heat pump field trial". In: *Applied Energy* 204 (2017), pp. 332 –342. ISSN: 0306-2619. DOI: https://doi.org/10.1016/j.apenergy.2017.07.026.

[51] Venkatesh Bala and Sanjeev Goyal. "Learning from Neighbours". In: *The Review of Economic Studies* 65.3 (July 1998), pp. 595–621. ISSN: 0034-6527. DOI: 10.1111/1467-937X.00059.

[52] Alex James et al. "Spatial utilization predicts animal social contact networks are not scale-free". In: *Royal Society Open Science* 4.12 (2017), p. 171209. DOI: 10.1098/rsos.171209. eprint: https://royalsocietypublishing.org/doi/pdf/10.1098/rsos.171209.

[53] International Organization for Standardization. *ISO 7730 2005-11-15 Ergonomics of the Thermal Environment: Analytical Determination and Interpretation of Thermal Comfort Using Calculation of the PMV and PPD Indices and Local Thermal Comfort Criteria*. International standards. ISO, 2005. URL: https://books.google.co.uk/books?id=p3YcoAEACAAJ.

[54] Marika Vellei et al. "The influence of relative humidity on adaptive thermal comfort". In: *Building and Environment* 124 (2017), pp. 171–185.

[55] Sanyogita Manu et al. "Field studies of thermal comfort across multiple climate zones for the subcontinent: India Model for Adaptive Comfort (IMAC)". In: *Building and Environment* 98 (2016), pp. 55–70.

[56] Antimo Barbato and Antonio Capone. "Optimization Models and Methods for Demand-Side Management of Residential Users: A Survey". In: *Energies* 7.9 (2014), 5787–5824. ISSN: 1996-1073. DOI: 10.3390/en7095787.

[57] Michael Diekerhof, Antonello Monti, and Sebastian Schwarz. *Chapter 12 - Demand-Side Management—Recent Aspects and Challenges of Optimization for an Efficient and Robust Demand-Side Management*. Academic Press, 2018, pp. 331 –360. ISBN: 978-0-12-812441-3. DOI: https://doi.org/10.1016/B978-0-12-812441-3.00012-4.

[58] Z. Wang, A. Scaglione, and R. J. Thomas. "Generating Statistically Correct Random Topologies for Testing Smart Grid Communication and Control Networks". In: *IEEE Transactions on Smart Grid* 1.1 (2010), pp. 28–39. ISSN: 1949-3061. DOI: 10.1109/TSG.2010.2044814.

[59] P Erdös and A Rényi. "On Random Graphs I". In: *Publicationes Mathematicae Debrecen* 6 (1959), pp. 290–297.

[60] Remco van der Hofstad. "Configuration Model". In: *Random Graphs and Complex Networks*. Vol. 1. Cambridge Series in Statistical and Probabilistic Mathematics. Cambridge University Press, 2016, 216–255. DOI: 10.1017/9781316779422.010.

[61] Michael Molloy and Bruce Reed. "A critical point for random graphs with a given degree sequence". In: *Random Structures & Algorithms* 6.2-3 (1995), pp. 161–180. DOI: 10.1002/rsa.3240060204.

[62] Edward A. Bender and E. Rodney Canfield. "The Asymptotic Number of Labeled Graphs with Given Degree Sequences". In: *Journal of Combinatorial Theory, Series A* 24.3 (1978), pp. 296–307. DOI: 10.1016/0097-3165(78)90059-6.

[63] Mark Newman. *Networks: An Introduction*. New York, NY, USA: Oxford University Press, Inc., 2010. ISBN: 0199206651, 9780199206650.

[64] Duncan J. Watts and Steven H. Strogatz. “Collective dynamics of ’small-world’ networks”. In: *Nature* 393.6684 (June 1998), pp. 440–442.

[65] Brian Hayes. “Computing Science: Graph Theory in Practice: Part II”. In: *American Scientist* 88.2 (2000), pp. 104–109.

[66] Valentino Crespi, Aram Galstyan, and Kristina Lerman. “Top-down vs bottom-up methodologies in multi-agent system design”. In: *Autonomous Robots* 24.3 (2008), pp. 303–313.

[67] Eric Bonabeau. “Agent-based modeling: Methods and techniques for simulating human systems”. In: *Proceedings of the National Academy of Sciences* 99.suppl 3 (2002), pp. 7280–7287. DOI: 10.1073/pnas.082080899.

[68] D. Hellbing and S. Ballietti. *Social Self-Organization, Understanding Complex Systems*. Springer-Verlag, 2012, pp. 25–70.

[69] M. Ventosa et al. “Electricity Markets modeling trends”. In: *Energy Policy* 33.7 (2005), pp. 897–913.

[70] Catherine S.E. Bale, Liz Varga, and Timothy J. Foxon. “Energy and complexity: New ways forward”. In: *Applied Energy* 138 (2015), pp. 150 –159. ISSN: 0306-2619. DOI: https://doi.org/10.1016/j.apenergy.2014.10.057.

[71] E. Kremers et al. “A Complex Systems Modelling Approach for Decentralised Simulation of Electrical Microgrids”. In: *Engineering of Complex Computer Systems (ICECCS), 2010 15th IEEE International Conference on*. 2010, pp. 302–311. DOI: 10.1109/ICECCS.2010.1.

[72] E. Chappin and G. Dijkema. “Agent-based modeling of energy infrastructure transitions”. In: *International Journal of Critical Infrastructures* 6.2 (2010), pp. 106–130.

[73] Gonzalez de Durana J. et al. “Agent based modeling of energy networks”. In: *Energy Conversion and Management* 82.0 (2014), pp. 308 –319. ISSN: 0196-8904. DOI: http://dx.doi.org/10.1016/j.enconman.2014.03.018.

[74] Z. Wang et al. “Customer-centered control system for intelligent and green building with heuristic optimization”. In: *2011 IEEE/PES Power Systems Conference and Exposition*. 2011, pp. 1–7.

[75] Desh Deepak Sharma, S.N. Singh, and Jeremy Lin. “Multi-agent based distributed control of distributed energy storages using load data”. In: *Journal of Energy Storage* 5 (2016), pp. 134–145.

[76] Menglian Zheng, Christoph J. Meinrenken, and Klaus S. Lackner. “Agent-based model for electricity consumption and storage to evaluate economic viability of tariff arbitrage for residential sector demand response”. In: *Applied Energy* 126 (2014), pp. 297–306. ISSN: 0306-2619. DOI: https://doi.org/10.1016/j.apenergy.2014.04.022.

[77] Perukrishnen Vytelingum et al. “Agent-based Micro-storage Management for the Smart Grid”. In: *Proceedings of the 9th International Conference on Autonomous Agents and Multiagent Systems: Volume 1 - Volume 1*. AAMAS ’10. Toronto, Canada: International Foundation for Autonomous Agents and Multiagent Systems, 2010, pp. 39–46.

[78] Zhu Wang et al. “Multi-agent control system with information fusion based comfort model for smart buildings”. In: *Applied Energy* 99 (2012), pp. 247–254. DOI: https://doi.org/10.1016/j.apenergy.2012.05.020.

[79] Johanna L. Mathieu et al. “Quantifying Changes in Building Electricity Use, with Application to Demand Response”. In: *IEEE Transactions on Smart Grid* (Nov. 2010).

[80] Chen Chen, Shalinee Kishore, and Lawrence V. Snyder. “An innovative RTP-based residential power scheduling scheme for smart grids”. In: *2011 IEEE International Conference on Acoustics, Speech and Signal Processing (ICASSP)* (2011), pp. 5956–5959.

[81] A. Jindal, M. Singh, and N. Kumar. “Consumption-Aware Data Analytical Demand Response Scheme for Peak Load Reduction in Smart Grid”. In: *IEEE Transactions on Industrial Electronics* 65.11 (2018), pp. 8993–9004.

[82] Steven F Railsback and Volker Grimm. *Agent-based and individual-based modeling: a practical introduction*. Princeton university press, 2019.

[83] Aric A. Hagberg, Daniel A. Schult, and Pieter J. Swart. "Exploring network structure, dynamics, and function using NetworkX". In: *Proceedings of the 7th Python in Science Conference (SciPy2008)*. Pasadena, CA USA, Aug. 2008, pp. 11–15.

[84] Dimitrios Michail et al. "JGraphT–A Java library for graph data structures and algorithms". In: *arXiv preprint arXiv:1904.08355* (2019).

[85] Michael J. North, Nicholson T. Collier, and Jerry R. Vos. "Experiences Creating Three Implementations of the Repast Agent Modeling Toolkit". In: *ACM Trans. Model. Comput. Simul.* 16.1 (Jan. 2006), pp. 1–25. ISSN: 1049-3301.

[86] Ian Richardson et al. "Domestic electricity use: a high-resolution energy demand model". English. In: *Energy and Buildings* 42.10 (Oct. 2010), pp. 1878–1887. ISSN: 0378-7788. DOI: 10.1016/j.enbuild.2010.05.023.

[87] SD Watson, Kevin J Lomas, and Richard A Buswell. "Decarbonising domestic heating: What is the peak GB demand?" In: *Energy policy* 126 (2019), pp. 533–544.

[88] Caroline Hughes and Sukumar Natarajan. "Summer thermal comfort and overheating in the elderly". In: *Building Services Engineering Research and Technology* 40.4 (2019), pp. 426–445. DOI: 10.1177/0143624419844518.

[89] Department for Business, Energy & Industrial Strategy. *Heat Network (Metering and Billing) Regulations 2014 Guidance for Estimating Heat Capacity*. https://assets.publishing.service.gov.uk/government/uploads/system/uploads/attachment_data/file/562787/Guidance_Heat_Estimator_Tool._January_2016__1_.docx. [Online; accessed 2020-09-22]. 2016.

[90] Dashamir Marini, Richard A Buswell, and Christina J Hopfe. "Sizing domestic air-source heat pump systems with thermal storage under varying electrical load shifting strategies". In: *Applied Energy* 255 (2019), p. 113811.